THEORETICAL INTERPRETATION ON D(π^+, K^+)X INCLUSIVE MISSING MASS SPECTRUM OF J-PARC E-27 EXPERIMENT

Hnin Hnin Hlaing @ Nu Nu Lwin[1], Theingi[2], Khin Swe Myint[3],
Yoshinori Akaishi[4], Toshimitsu Yamazaki[5]

Abstract

In this research work, the inclusive missing-mass spectrum of D(π^+, K^+)X reaction at J-PARC E-27 experiment have been studied. J-PARC E27 experiment was conducted to search for the simplest kaonic nuclear bound state by using D(π^+, K^+)X reaction at the beam momentum of 1.7 GeV/c. In the E-27 experiment, high energy pion is incident upon deuteron target and interacts with neutron in the target to produce K^+, K^- and p. Due to the strong attractive force between K^- and p, Λ^* = Λ(1405) is formed as a doorway state to populate K^-pp. The missing mass spectrum obtained from E-27 experiment at J-PARC has covered energy regions of quasi free Λ-p, Σ-p, Λ^*-p, Σ^*-p production and K^-pp bound state. The missing mass spectrum of D(π^+, K^+)X reaction covering all the above energy regions have been analyzed by using Green's function method.

Keywords: Λ (1405) doorway state, quasi-free, inclusive spectrum.

Introduction

The theoretical predictions of possible existence of deeply bound $\overline{K}$ nuclear states in light nuclei have been proposed theoretically by Akasishi and Yamazaki (Akaishi, Y., and Yamazaki, T. (1999)). They constructed $\overline{K}N$ interactions phenomenologically so as to reproduce low energy $\overline{K}N$ scattering data, kaonic hydrogen atom data and the binding energy and decay width of Λ(1405), which is asserted to be an I = 0 quasi-bound state of $\overline{K}N$. These interactions are characterized by a strongly attractive I = 0 part. Yamazaki and Akaishi (Akaishi, Y., and Yamazaki, T. (2002) & Akaishi, Y., and Yamazaki,

1. Physics Department, Mandalay University of Distance Education, Mandalay, Myanmar
2. Physics Department, , Mandalay University, Mandalay, Myanmar
3. Physics Department, Mandalay University, Mandalay, Myanmar
4. RIKEN, Nishina Center, Wako, Saitama 351-0198, Japan
5. Department of Physics, University of Tokyo, Bunkyo-ku, Tokyo 113-0033, Japan

T. (2002)) have predicted the possible existence of nuclear $\overline{K}$ bound states with narrow widths in (pp), ^{3}He , ^{4}He and ^{8}Be.

Moreover, the importance of the three body dynamics in predicting the resonance energy of strange dibaryon $\overline{K}NN$ has been investigated by Ikeda and Sato (Ikeda, Y., and Sato,T. (2007)). The binding energy for $\overline{K}NN$ is obtained to be 60-95 MeV and width to be 45-80 MeV by employing the $\overline{K}N - \pi\Sigma$ interaction based on the chiral lagrangian.

In search for quasi bound states in the $K^{-}pp$ system, the three-body $\overline{K}NN$ and $\pi\Sigma N$ coupled channel Faddeev calculation was also studied by Shevchenko et al. (Shevchenko, N.V., Gal, A., and Mares, J. (2007)). It should be noted that, even for the simplest kaonic nuclear system ($K^{-}pp$ system), different computation techniques and different $\overline{K}N$ interactions, have produced controversial results. These controversial theoretical issues have led to intensify the experimental search for kaonic nuclear systems.

Among the number of experimental searches for the simplest kaonic nucleus, FINUDA collaboration at DAΦNE (Agnello, M. *et al*., (2005)) first reported an observation of the $K^{-}pp$ bound state. They investigated the stopped K^{-} reaction on several kinds of target and observed a number of Λp pairs emitted in back to back. They observed a bump structure in the invariant mass spectrum of these Λp pairs from the ^{6}Li, ^{7}Li and ^{12}C targets. By assuming that this structure is due to the $K^{-}pp$ bound state, the binding energy and the decay width were evaluated to be 115^{+6}_{-5} (stat) $^{+3}_{-4}$ (syst) MeV and 67^{+14}_{-11} (stat) $^{+2}_{-3}$ (syst) MeV, respectively, which is more binding than the previously mentioned theoretical values.

Another positive result of the $K^{-}pp$ bound state was also reported by the DISTO collaboration at SATURNE (Yamazaki, T. *et al*., (2010)). They reanalyzed the data set of the $p+ p \rightarrow \Lambda + p + \vec{q}_2$ reaction at T_p= 2.85 GeV and observed a bump structure in ΔM_{K^+} missing mass and $M_{p\Lambda}$ invariant mass spectra in large transverse momentum of protons and kaons. The binding

energy and decay width were determined as 103 ± 3(stat) $\pm$ 5(syst) MeV and 118 ± 8 (stat) $\pm$ 10(syst) MeV, respectively. In this case the level width is much larger than that of FINUDA. Very recently, J-PARC E-27 experiment was carried out in an attempt to settle this controversial issue.

The J-PARC E-27 experiment has been proposed to search for the K^-pp bound state by using the (π^+, K^+) reaction on a liquid deuterium target at 1.7 GeV/c (Ichikawa, Y. *et al.,* (2013) & Ichikawa, Y. *et al.,* (2015)). In this experiment, there are many background processes of quasi-free hyperon production such as Λ, Σ, Λ (1405) and Σ(1385) and the signal of K^-pp was predicted to be small compared with the background (Yamazaki, T. *et al.,* (2007) & Akaishi, Y., Dote, A., and Yamazaki, T. (2005)). It was difficult to be observed in inclusive measurements. Therefore, coincidence of a proton from the decay of K^-pp was required to suppress these backgrounds. They have reported a broad peak structure around 2.27 GeV/c^2 in a proton-coincidence spectrum , which is attributed to the K^-pp bound state. Our purpose is to interpret theoretically inclusive missing-mass spectrum from the E-27 experiment. So, we have calculated missing mass spectrum of the E-27 production reaction by using Green's function method.

Mathematical Formulation of Reaction Cross Section

This section is the mathematical formulations of missing mass spectrum of D(π^+, K^+) reaction. In this section, we have calculated transition matrix and differential cross section for this reaction by using Green's function method. A schematic diagram of the reaction mechanism is shown in Fig (1).

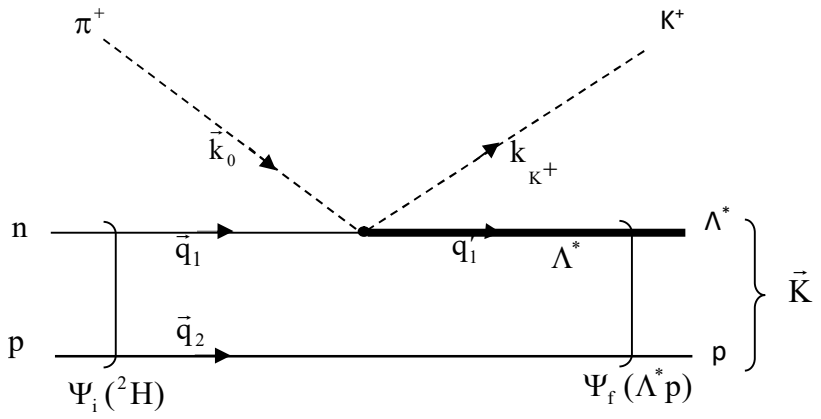

Figure1. Schematic diagram of the $D(\pi^+, K^+)X$ reaction.

Transition Matrix

We can write transition matrix between the initial state $\pi^+ + D$ and the final state $K^+ + \Lambda^* p$ of Fig (1).

$$T_{fi}^{(n)} = \left\langle \Psi_f^n,\ \vec{K},\ \vec{k}_{K^+} \middle| T \middle|\ \vec{k}_0,\ 0,\ \Psi_i \right\rangle \tag{1}$$

Equation (1) becomes

$$T_{fi}^{(n)} = \left(\frac{L}{2\pi}\right)^9 \int d\vec{q}_1 \int d\vec{q}_2 \int d\vec{q}_1' \left\langle \Psi_f^n, \vec{K} \middle| \vec{q}_2, \vec{q}_1' \right\rangle \left[\vec{k}_{K^+}, \vec{q}_1' \middle| T \middle| \vec{k}_0, \vec{q}_1 \right] \left[\vec{q}_1, \vec{q}_2 \middle| 0, \Psi_i \right\rangle \tag{2}$$

We can write this equation in terms of relative momentum and center of mass momentum.

Therefore, equation (2) is rewritten as

$$T_{fi}^{(n)} = \left(\frac{L}{2\pi}\right)^9 \int d\vec{q}_1 \int d\vec{q}_2 \int d\vec{q}_1' \left\langle \Psi_f^n, \vec{K} \middle| \vec{\tilde{q}}', \vec{Q}' \right\rangle \left[\vec{q}_1', \vec{k}_{K^+} \middle| T \middle| \vec{q}_1, \vec{k}_0 \right] \left[\vec{q} \middle|\ \Psi_i \right\rangle \left[\vec{Q} \middle| 0 \right] \tag{3}$$

with relative momentum between neutron and pion $\vec{\tilde{q}}_1 = \dfrac{M_n \vec{k}_0 - m_{\pi^+} \vec{q}_1}{M_n + m_{\pi^+}}$

relative momentum between neutron and proton $\vec{\tilde{q}} = \dfrac{M_p \vec{q}_1 - M_n \vec{q}_2}{M_n + M_p}$

relative momentum between Λ^* and proton $\vec{\tilde{q}}' = \dfrac{M_{\Lambda^*} \vec{q}_2 - M_p \vec{q}_1'}{M_{\Lambda^*} + M_p}$

relative momentum between Λ^* and kaon $\vec{\tilde{q}}_1' = \dfrac{M_{\Lambda^*} \vec{k}_{K^+} - M_{K^+} \vec{q}_1'}{M_{\Lambda^*} + M_{K^+}}$

Center of mass momentum of Λ^* and proton $\vec{Q}' = \vec{q}_2 + \vec{q}_1'$

and the center of mass momentum of neutron and proton $\vec{Q} = \vec{q}_1 + \vec{q}_2$

Ψ_i and Ψ_f are described by relative momentum only center of mass motion is not affected.

Therefore, equation (3) becomes,

$$T_{fi}^{(n)} = \left(\frac{L}{2\pi}\right)^9 \int d\vec{q}_1 \int d\vec{q}_2 \int d\vec{q}_1' \overbrace{\left\langle \Psi_f^n \left| \vec{\tilde{q}}' \right.\right]}^{1} \overbrace{\left[\vec{K} \left| \vec{Q}' \right.\right]}^{2} \overbrace{\left[\vec{\tilde{q}}_1' \left| t_{\pi n} \right| \vec{\tilde{q}}_1 \right]}^{3} \overbrace{\left[k_{K^+} + \vec{q}_1' \left| \vec{k}_0 + \vec{q}_1 \right.\right]}^{4}$$

$$\times \overbrace{\left[\vec{\tilde{q}} \left| \Psi_i \right\rangle\right]}^{5} \overbrace{\left[\vec{Q} \left| 0 \right.\right]}^{6} \qquad (4)$$

Equation (4) becomes,

$$T_{fi}^{(n)} = \int d\vec{q}_1 \int d\vec{q}_2 \int d\vec{q}_1' \left\langle \Psi_f^n \left| \vec{\tilde{q}}' \right.\right] \delta(\vec{K} - \vec{Q}') \left[\vec{\tilde{q}}_1' \left| t_{\pi n} \right| \vec{\tilde{q}}_1 \right] \delta(\vec{k}_{K^+} + \vec{q}_1' - \vec{k}_0 - \vec{q}_1) \times \left[\vec{\tilde{q}} \left| \Psi_i \right\rangle \delta(\vec{Q}) \right. \qquad (5)$$

By integrating equation (5) with respect to $d\vec{q}_1'$,

$$T_{fi}^{(n)} = \overbrace{\int d\vec{q}_1 \int d\vec{q}_2}^{d\vec{\tilde{q}}\, d\vec{Q}} \left\langle \Psi_f^n \left| \vec{\tilde{q}}' \right. \right] \delta\left(\vec{k}_{K^+} + \vec{K} - \vec{q}_2 - \vec{k}_0 - \vec{q}_1 \right) \left[\vec{\tilde{q}}_1' \left| t_{\pi n} \right| \vec{\tilde{q}}_1 \right] \left[\vec{\tilde{q}} \right| \Psi_i \rangle \delta(\vec{Q}) \qquad (6)$$

After performing the integration with respect to $d\vec{Q}$, we obtained

$$T_{fi}^{(n)} = \delta\left(\vec{K} + \vec{k}_{K^+} - \vec{k}_0 \right) \int d\vec{\tilde{q}} \left\langle \Psi_f^n \left| \vec{\tilde{q}}' \right. \right] \left[\vec{\tilde{q}}_1' \left| t_{\pi n} \right| \vec{\tilde{q}}_1 \right] \left[\vec{\tilde{q}} \right| \Psi_i \rangle \qquad (7)$$

where $\left[\vec{\tilde{q}}_1' \left| t_{\pi n} \right| \vec{\tilde{q}}_1 \right]$ is the two-body t-matrix for the elementary process $\pi^+ + n \rightarrow K^+ + \Lambda^*$.

Differential Cross Section

Differential cross section of $D(\pi^+, K^+)X$ is calculated as;

$$d^6\sigma = \frac{L^3}{v_0} \frac{2\pi}{\hbar} \sum_n \delta\left(E_i - E_f^n \right) \left(\frac{L}{2\pi} \right)^3 d\vec{k}_{K^+} \left(\frac{L}{2\pi} \right)^3 d\vec{K} \left| T_{fi}^{(n)} \right|^2 \qquad (8)$$

where, $d^6\sigma =$ the probability of producing this reaction with the emitted particle momentum between $\vec{k}_{K^+}$ and $\vec{k}_{K^+} + d\vec{k}_{K^+}$ and with the kaonic nucleus momentum between $\vec{K}$ and $\vec{K} + d\vec{K}$.

$\frac{v_0}{L^3}$ = incident flux, $v_0 = \frac{\hbar k_0 c^2}{E_0}$ = incident kaon velocity

$\delta(E_i - E_f^n)$ = energy conservation term

$\left(\frac{L}{2\pi} \right)^3 d\vec{k}_{K^+} \left(\frac{L}{2\pi} \right)^3 d\vec{K}$ = phase volume (or) phase space

By substituting equation (7) in equation (8), equation (8) becomes,

$$d^6\sigma = \frac{L^3}{v_0}\frac{2\pi}{\hbar}\sum_n \delta\left(E_i - E_f^n\right)\left(\frac{L}{2\pi}\right)^3 d\vec{k}_{K^+}\left(\frac{L}{2\pi}\right)^3 d\vec{K}$$

$$\times\delta^2\left(\vec{K} + \vec{k}_{K^+} - \vec{k}_0\right)\left|\int d\vec{\tilde{q}}\left\langle\Psi_f^n\left|\vec{\tilde{q}}'\right.\right]\left[\vec{\tilde{q}}_l'\left|t_{\pi n}\right|\vec{\tilde{q}}_l\right]\left[\vec{\tilde{q}}\left|\Psi_i\right.\right\rangle\right|^2 \qquad (9)$$

By integrating equation (9) with $d\vec{K}$, we get

$$d^3\sigma = \frac{(2\pi)^4}{\hbar^2 k_0 c^2}E_0\left|\left\langle t_{\pi n}\right\rangle\right|^2 d\vec{k}_{K^+}\sum_n \delta\left(E_i - E_f^n\right)\left|\int d\vec{\tilde{q}}\left\langle\Psi_f^n\left|\vec{\tilde{q}}'\right.\right]\left[\vec{\tilde{q}}\left|\Psi_i\right.\right\rangle\right|^2 \qquad (10)$$

by taking an averaged value $\left\langle t_{\pi n}\right\rangle$ as an approximation of $\left[\vec{\tilde{q}}_l'\left|t_{\pi n}\right|\vec{\tilde{q}}_l\right]$. Now we are going to solve the energy conservation term $\sum_n \delta(E_i - E_f^n)$.

Energy of initial state, $E_i = E_0 + M_n c^2 + M_P c^2 - BE(^2H)$

Energy of final state,

$$E_f^n = E_{K^+} + (M_{\Lambda^*} c^2 + M_p c^2) + \left\langle\Psi_f^n\left|H_{\Lambda^* p}\right|\Psi_f^n\right\rangle + \frac{\hbar^2}{2(M_{K^- pp})}(\vec{k}_0 - \vec{k}_{K^+})^2$$

where $\dfrac{\hbar^2(\vec{k}_0 - \vec{k}_{K^+})^2}{2(M_{K^- pp})}$ = recoil energy of the product nucleus

$\left\langle\Psi_f^n\left|H_{\Lambda^* p}\right|\Psi_f^n\right\rangle$ = excitation energy of final state

Then $E_i - E_f^n$ is rewritten as;

$$E_i - E_f^n = E - \left\langle\Psi_f^n\left|H_{\Lambda^* p}\right|\Psi_f^n\right\rangle$$

where

$$E=(E_0-E_{K^+})+(M_nc^2-M_{\Lambda^*}c^2)-BE(^2H)-\frac{\hbar^2}{2(M_{K^-pp})}(\vec{k}_0-\vec{k}_{K^+})^2$$

$\delta(E_i-E_f^n)$ is expressed as, $\delta(E_i-E_f^n)=\left\langle\Psi_f^n\left|\delta(E_i-E_f^n)\right|\Psi_f^n\right\rangle$

$$\delta(E_i-E_f^n)=\left(-\frac{1}{\pi}\right)\mathrm{Im}\left\langle\Psi_f^n\left|\frac{1}{E-H_{\Lambda^*p}+i\varepsilon}\right|\Psi_f^n\right\rangle$$

The following term consists in the right hand side of equation (10) rewritten as

$$\sum_n\delta(E_i-E_f^n)\left|\int d\vec{\tilde{q}}\left\langle\Psi_f^n\middle|\vec{\tilde{q}}'\right\rangle\left\langle\vec{\tilde{q}}\middle|\Psi_i\right\rangle\right|^2=$$
$$\left(-\frac{1}{\pi}\right)\mathrm{Im}\int d\vec{r}\int d\vec{r}'\,f^*(\vec{r}')\left\langle\vec{r}'\right|\frac{1}{E-H_{\Lambda^*p}+i\varepsilon}\left|\vec{r}\right\rangle f(\vec{r}) \qquad (11)$$

where $f(\vec{r})=e^{-i\eta(\vec{k}_0-\vec{k}_{K^+})\vec{r}}$ $\Psi_i(\vec{r})=e^{i\vec{Q}\vec{r}}\frac{u_i(r)}{r}\frac{1}{\sqrt{4\pi}}$ with $\eta=\frac{M_p}{M_p+M_{\Lambda^*}}$

$$f^*(\vec{r}')=e^{-i\eta(\vec{k}_0-\vec{k}_{K^+})\vec{r}}\quad\Psi_i^*(\vec{r}')=e^{-i\vec{Q}\vec{r}}\frac{u_i^*(r')}{r'}\frac{1}{\sqrt{4\pi}}$$

$\Psi_i(\vec{r})$ = wave function of the target nucleus

Substituting equation (11) in equation (10) and it becomes,

$$d^3\sigma=\frac{(2\pi)^4}{\hbar^2k_0c^2}E_0\left|\left\langle t_{\pi n}\right\rangle\right|^2k_{K^+}^2\,dk_{K^+}\,2\pi d\cos\theta_k\left(-\frac{1}{\pi}\right)$$
$$\times\mathrm{Im}\left[\int d\vec{r}\int d\vec{r}'\,f^*(\vec{r}')\left\langle\vec{r}'\left|\frac{1}{E-H_{\Lambda^*p}+i\varepsilon}\right|\vec{r}\right\rangle f(\vec{r})\right] \qquad (12)$$

The final differential cross-section for missing-mass spectrum of the $D(\pi^+, K^+)X$ reaction is given by

$$\frac{d^2\sigma}{dY c^2 d\cos\theta_K} = \frac{(2\pi)^5}{\hbar^2 k_0 c^2} E_0 \frac{k_{K^+} \left|\langle t_{\pi n}\rangle\right|^2}{\left\{\frac{\hbar^2 c^2}{E_{K^+}} + \frac{\hbar^2}{M_{K^- pp}}\left(1 - \frac{k_0}{k_{K^+}}\cos\theta_{K^+}\right)\right\}} \times\left(-\frac{1}{\pi}\right) \mathrm{Im}\left[\int d\vec{r}\int d\vec{r}\,' f^*(\vec{r}\,')\langle\vec{r}\,'| \frac{1}{E - H_{\Lambda^* p} + i\varepsilon}|\vec{r}\rangle f(\vec{r})\right] \tag{13}$$

where the first term $\frac{(2\pi)^5}{\hbar^2 k_0 c^2} E_0 \frac{k_{K^+} \left|\langle t_{\pi n}\rangle\right|^2}{\left\{\frac{\hbar^2 c^2}{E_{K^+}} + \frac{\hbar^2}{M_{K^- pp}}\left(1 - \frac{k_0}{k_{K^+}}\cos\theta_{K^+}\right)\right\}}$ is the kinematical factor and

the second term $\left(-\frac{1}{\pi}\right) \mathrm{Im}\left[\int d\vec{r}\,'\int d\vec{r}\, f^*(\vec{r}\,')\langle\vec{r}\,'| \frac{1}{E - H_{\Lambda^* p} + i\varepsilon}|\vec{r}\rangle f(\vec{r})\right]$ is the spectral function $S(E)$.

The spectral function $S(E)$ contains Green's function $\left\langle \vec{r}\,' \left| \frac{1}{E - H_{\Lambda^* p} + i\varepsilon} \right| \vec{r} \right\rangle$.

Green-function in coordinate representation is

$$G^+(\vec{r}\,', \vec{r}) = \left\langle \vec{r}\,' \left| \frac{1}{E - H_{\Lambda^* p} + i\varepsilon} \right| \vec{r} \right\rangle$$

where $H_{\Lambda^* p} = T_{\Lambda^* p}$ and $V_{\Lambda^* p}$. $H_{\Lambda^* p}$ is the Hamiltonian of Λ^* p.

The coordinate representation of Green's function $G^{+}(\vec{r}',\vec{r})$ which obey

$$\left\{E - H_{\Lambda^* p}\right\} G^{+}(\vec{r}',\vec{r}) = \left\langle \vec{r}' \left| \frac{1}{E - H_{\Lambda^* p} + i\varepsilon} \right| \vec{r} \right\rangle = \delta(\vec{r}' - \vec{r})$$

Green function and delta function are expressed in partial wave expansion as follows;

$$G^{+}(\vec{r}',\vec{r}) = \sum_{\ell=0}^{\infty} \sum_{M} Y_{\ell M}(\hat{\vec{r}}) \frac{G_{\ell}^{+}(r',r)}{rr'} Y_{\ell M}^{*}(\hat{\vec{r}}') \tag{14}$$

$$\delta(\vec{r}' - \vec{r}) = \sum_{\ell=0}^{\infty} \sum_{M} Y_{\ell M}(\hat{\vec{r}}) \frac{\delta(r' - r,)}{rr'} Y_{\ell M}^{*}(\hat{\vec{r}}') \tag{15}$$

Then the radial part of the Green's function $G_{\ell}^{+}(\vec{r}',\vec{r})$ is satisfied by solving the following equation;

$$\left[k^2 + \frac{d^2}{dr^2} - \frac{\ell(\ell+1)}{r^2} - \tilde{U}(r)\right] G_{\ell}^{+}(r',r) = \frac{2\mu}{\hbar^2} \delta(\vec{r}' - \vec{r})$$

$k^2 = \frac{2\mu E}{\hbar^2}$, $\tilde{U}(r) = \frac{2\mu}{\hbar^2} V_{\Lambda^* p}(r)$ is the potential between Λ^* and p.

We can write the radial part of the Green's function in the following form;

$$G^{+}(r',r) = G_{\ell 1}^{+}(r',r) = C_1 u_{\ell}^{0}(r) \quad \text{for } (0 < r < r')$$

$$G_{\ell 2}^{+}(r',r) = C_2 u_{\ell}^{+}(r) \quad \text{for } (r' < r < \infty)$$

We have prepared the two solutions of

$\left[k^2 + \frac{d^2}{dr^2} - \frac{\ell(\ell+1)}{r^2} - \tilde{U}(\vec{r})\right] u(r) = 0$, with the boundary conditions

$$u_{\ell}^{0}(0) \xrightarrow{r \to 0} 0 \qquad \text{for } u_{\ell}^{0}(r)$$

$$u_{\ell}^{+}(0) \xrightarrow{r \to \infty} kr\, h_{\ell}^{+}(kr) \qquad \text{for } u_{\ell}^{+}(r)$$

We have $C_1 u_\ell^{(0)}(r') - C_2 u_\ell^{(+)}(r') = 0$

$$C_1 u_\ell^{(0)'}(r') - C_2 u_\ell^{(+)'}(r') = \frac{2\mu}{\hbar^2}$$

We get two parts of the radial part Green's function as

$$G_{\ell 1}^{+}(r',r) = \frac{2\mu}{\hbar^2} \frac{u_\ell^{(+)}(r') u_\ell^{(0)}(r)}{W(u_\ell^{(0)}, u_\ell^{(+)})} \tag{16}$$

$$G_{\ell 2}^{+}(r',r) = \frac{2\mu}{\hbar^2} \frac{u_\ell^{(0)}(r') u_\ell^{(+)}(r)}{W(u_\ell^{(0)}, u_\ell^{(+)})} \tag{17}$$

We combine the equation (16) and (17)

$$G_\ell^{+}(r',r) = \frac{2\mu}{\hbar^2} \frac{u_\ell^{(+)}(r_>) u_\ell^{(0)}(r_<)}{W(u_\ell^{(0)}, u_\ell^{(+)})} \tag{18}$$

Substituting the equation (18) into equation (14), we get

$$G^{(+)}(r',r) = \frac{2\mu}{\hbar^2} \sum_{\ell=0}^{\infty} \sum_{M} Y_{\ell M}(\hat{\vec{r}}) \frac{u_\ell^{(+)}(r_>) u_\ell^{(0)}(r_<)}{rr' W(u_\ell^{(0)}, u_\ell^{(+)})} Y_{\ell M}^{*}(\hat{\vec{r}}') \tag{19}$$

By substituting the above equation into equation (13), we obtained the final expression as follows;

$$\frac{d^2\sigma}{dY_{\vec{c}}.d\cos\theta_{K^+}} = \frac{(2\pi)^5}{\hbar^2 k_0 c^2} \frac{E_0 \vec{k}_{K^+} \left| \langle t_{\pi n} \rangle \right|^2}{\left\{ \frac{\hbar^2 c^2}{E_{K^+}} + \frac{\hbar^2}{M_{K^- pp}} \left(1 - \frac{k_0}{k_{K^+}} \cos\theta_{K^+}\right) \right\}} \times \left(-\frac{1}{\pi}\right) \mathrm{Im} \left[\sum_{\ell=0}^{\infty} (2\ell+1) \int dr' \int dr j_\ell^{*}(Qr') u_i^{*}(r') \frac{u_\ell^{0}(r_<) u_\ell^{+}(r_>)}{W(u_\ell^{0}, u_\ell^{+})} j_\ell(Qr) u_i(r) \right] \tag{20}$$

Results and Discussions

Study on the Quasi-Free Region with Fermi Motion Consideration

We have studied the quasi-free regions namely Λ-p, Σ-p and Λ^*-p, Σ^*-p of the E-27 inclusive spectrum. In order to understand the origins of quasi-free Λ-p, Σ-p, Λ^*-p, Σ^*-p structure, we firstly determine the peak positions and level widths by considering the Fermi motion of neutron in target deuteron. The neutron momentum distribution is taken into account in determining the emitted kaon momentum from which the missing mass of K^-pp is obtained using the relation $M_X c^2 = \sqrt{(E_{init} - E_{obs})^2 - (p_{init} - p_{obs})^2 c^2}$. We have used the neutron momentum distribution in deuteron as Fermi type and neutron is assumed to be the off-shell mass as $M^{*2}_n = \left(M_D - \sqrt{M_p^2 + p_n^2}\right)^2 - p_n^2$. Our calculated peak structures of quasi-free production are shown in Figs. (1 - 4) and Table (1). According to our calculations it is found that Λ-p and Σ-p peaks are in good agreement with experimental positions but Λ^*-p and Σ^*- p peaks are quite different from the experimental positions.

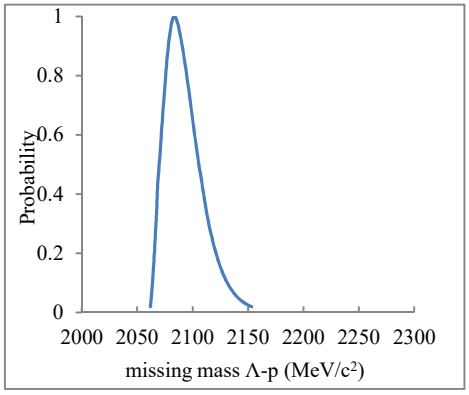

Figure 1. Quasi – free Λ-p production spectrum due to Fermi motion

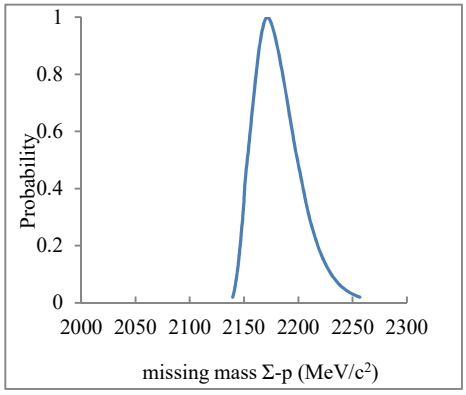

Figure 2. Quasi–free Σ-p production spectrum due to Fermi motion

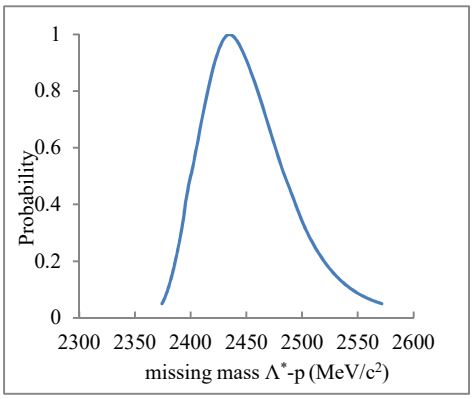

Figure 3. Quasi –free Λ^*-p production spectrum due to Fermi motion

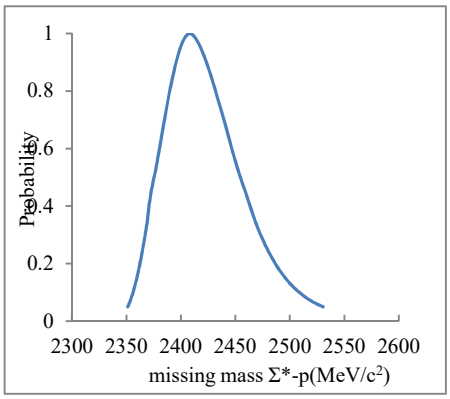

Figure 4. Quasi –free Σ^*-p production spectrum due to Fermi motion

Table 1. The experimental and calculated peak positions and levelwidths for quasi-free process.

Quasi-free production	**Peak position Calculated (MeV/c²)**	**Peak position Experimental (MeV/c²)**	**Level width Calculated (MeV/c²)**	**Level width Experimental (MeV/c²)**
Λ-p	2083.6	2085	35.8	50
Σ- p	2171.53	2170	47.5	45
Λ^*-p	2434.85	2389	80	80
Σ^*- p	2408.22	2389	78	80

Inclusive Missing Mass Spectrum of D(π^+, K^+)X Reaction

We have studied the quasi-free regions of the inclusive missing mass spectrum for D(π^+, K^+)X reaction from J-PARC E-27. We have calculated the missing mass spectrum of this reaction by employing YA and DISTO potential for Y-p (Λ-p and Σ-p) and Y^*-p (Λ^*-p and Σ^*- p) interactions. In the regions of Λ-p and Σ-p, the following optical potential is used;

$$V^{opt}(r) = 5000.0 \exp\left[-\left(\frac{r}{0.4}\right)^2\right] - (V_0 f_R + i W_0 f_I) \exp\left[-(r/1.0)^2\right] \text{with}$$

V_0 = -272.6 MeV, W_0 = -47 MeV and f_R = 0.5, f_I= 0.0 for Λp and f_R = 0.9,

f_I = 1.0 for Σp. It is found that the missing mass spectrum of quasi-free Λ-p production in Fig (5). The peak position and level width are 2083.9 MeV/c^2 and 35.8 MeV. Similarly, Fig.(6) shows the missing mass spectrum of quasi-free Σ-p production. The peak position and level width are found to be 2167.6 MeV/c^2 and 47.5 MeV.

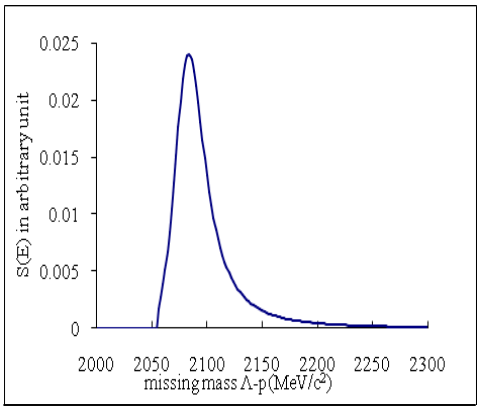

Figure 5. Missing mass spectrum of quasi-free Λ-p production.

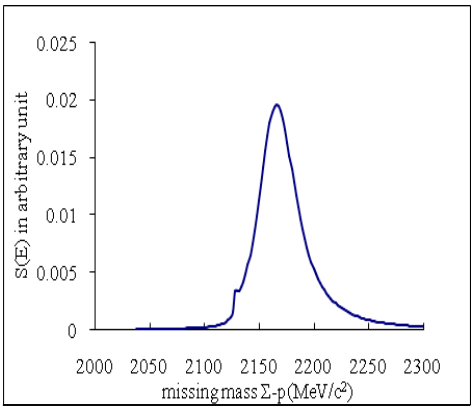

Figure 6. Missing mass spectrum of quasi-free Σ-p production.

In order to see the effect of quasi-free Λ^*-p production on the formation region, we have switched off the Λ^*-p interaction in our calculation. We have considered two cases which are (i) without including the level width of Λ^* and (ii) including the level width of Λ^*. Fig.(7) shows the missing mass spectrum of quasi free Λ^*-p production. The red curve is the missing mass spectrum of quasi free Λ^*-p production for the first case where the level width of Λ^* is not included. It can be seen that the peak position is 2435.4 MeV/c^2 and level width is 90 MeV. The blue curve is the missing mass spectrum of quasi free Λ^*-p production for the second case. The peak position and level width of Λ^*- p are found to be 2423.4 MeV/c^2 and 170 MeV respectively. The effect of Γ_{Λ^*} is slightly shifting the peak position to the lower mass energy region and increasing the level width by 80 MeV.

And then, we have investigated the missing-mass spectrum of the quasi-free Σ^*-p region by turning off the Σ^*-p interaction. We have found the similar characteristics as that of the Λ^*-p. The calculated missing mass spectrum of quasi-free Σ^*-p production is displayed in Fig. (8). The green

curve represented the missing mass spectrum of quasi-free Σ^*-p production which is obtained by giving the level width to be zero. It is found that the peak position and level width are 2405.2MeV/c^2 and 70.5 MeV, respectively. When the level width of Σ^* is taken to be 36 MeV, the peak position is 2403.2 MeV/c^2 and its width becomes 90 MeV, shown by orange curve. It is seen that the peak position remains unchanged while the level width increases by nearly 20 MeV.

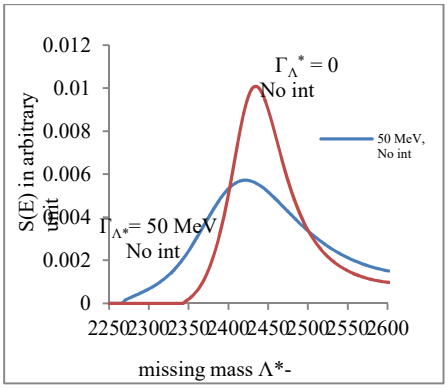

Figure 7. Missing mass spectrum of quasi-free Λ^*-p production; (i) red curve is with Γ_{Λ}^* = 0 and without interaction (ii) blue curve is with Γ_{Λ}^*=50 MeV and without interaction

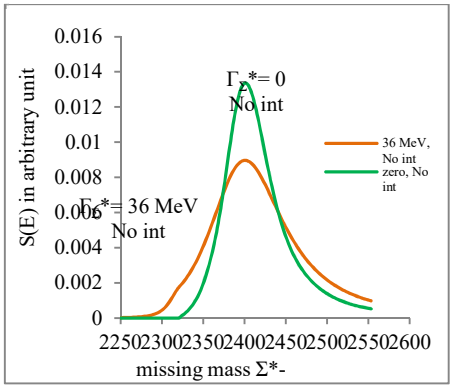

Figure 8. Missing mass spectrum of quasi-free Σ^*-p production; (i) green curve is with Γ_{Σ}^*= 0 and without interaction (ii) orange curve is with Γ_{Σ}^*=36 MeV and without interaction

In order to obtain the missing mass spectrum covering all regions of quasi-free Λ-p, Σ-p, Λ^*-p and Σ^*-p as given in the experimental spectrum, we have combined the above mentioned spectra into one spectrum Fig (9).

The upper right of the Fig (9) shows the experimental missing mass spectrum to be compared with our calculated spectrum. In the Y-p region, our calculated spectrum has a cusp peak in 2130 MeV/c^2 at the Σ-p threshold which agrees very well with the experimental curve. Our calculated spectrum well reproduced the missing mass spectrum of E-27 experiment including the cusp peak in 2130 MeV/c^2 due to $\Sigma N \rightarrow \Lambda N$ conversion in the Y-p region. In the Y^*-p region, our peak is about 30 MeV shifted to the higher mass region compared to the experimental curve. It can be seen from the experimental

spectrum and from the calculated spectrum, there are large quasi-free regions which may obscure the small signal of K^-pp bound state.

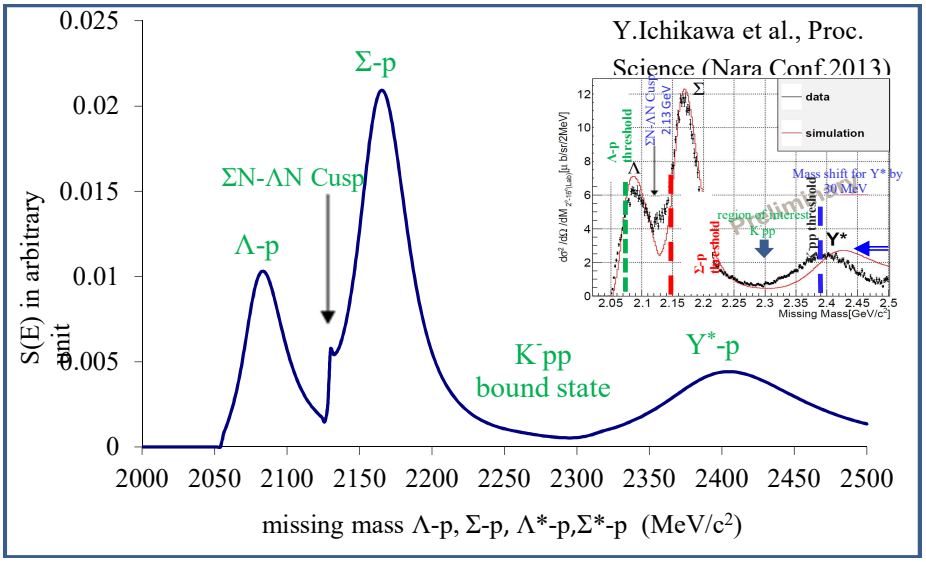

Figure 9. Missing mass spectrum of quasi-free Λ-p, Σ-p, Λ^*-p, Σ^*-p production.

We have obtained the missing mass spectrum of Λ^*p production by employing DISTO potential for Λ^*-p interaction. In our calculation, we used the Λ^*-p interaction which has the following form

$$V_{Y^*p}^{opt}(r)=(V_0+iW_0)\left(\frac{r}{c}\right)^2 \exp\left[-(r/c)\right] \quad \text{where} \quad V_0= -394.0 \text{ MeV},$$

W_0= -95.0 MeV are potential strength parameter and c = 0.3 fm is range parameter for DISTO Λ^*-p interaction. The Λ^*p DISTO interaction is obtained by enhancing the YA interaction by 17% which is attributed to partial restoration of chiral symmetry. We have calculated the missing mass spectrum of Λ^*p production with angular momentum contributions for l = 0, l = 1 to l = 4 to study their effect on the production spectrum. Fig. (10) displayed the missing mass spectrum of Λ^*p. It can be found that the peak position at l = 0 indicates the bound state region below the Λ^*p threshold. The peak position at

l = 1 to l = 4 are found in the energy region above the Λ^*p threshold. Thus, quasi-free region is dominated by the higher angular momentum contributions.

Similarly, we have calculated the missing mass spectrum of Λ^* - p production with angular momentum contributions for l_{min} = 0, l_{max} = 1 to l_{max} = 4. In the Fig.(11), the peak position of the bound state region dominates at l_{min} = 0 to l_{max} = 0 below the threshold while the peak position of the quasi-free region dominates at l_{min} = 0, l_{max} = 1 to l_{max} = 4 above the threshold. The peak at the l = 0 is clearly seen bound state. However, it is almost obscured by the large background of quasi-free Λ^*p production, which can be seen in Fig.(11). The quasi-free Λ^*-p production is dominant in higher angular momentum contributions.

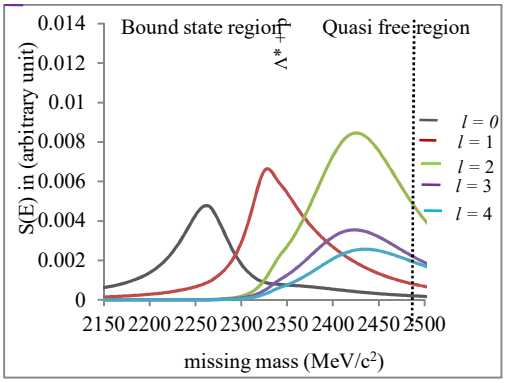

Figure 10. Missing mass spectrum of Λ^*p with individual angular momentum contribution

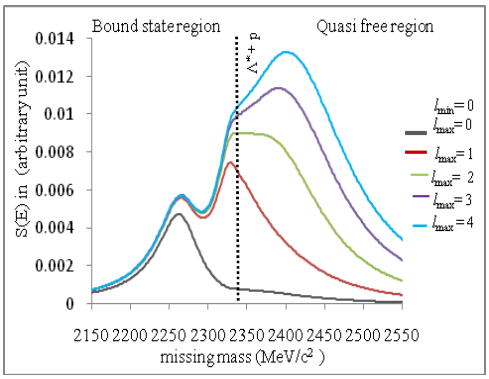

Figure11. Missing mass spectrum of Λ^*p with total angular momentum contribution

Conclusion

We studied the inclusive missing mass spectrum of D(π^+, K^+)X reaction from J-PARC E 27 experiment which covers all energy regions of quasi free Y-p (Λ-p, Σ-p), Y^*-p (Λ^*-p, Σ^*-p) production and K^-pp bound state. In order to understand the origins of these quasi-free Y-p and Y^*-p structure, we have investigated the nature of the background processes which are quasi-free regions namely Y-p (Λ-p, Σ-p) and Y^*p (Λ^*-p, Σ^*-p). In our simple consideration, level widths of Λ^* and Σ^* are not taken into account which

might be the discrepancy between our calculated values and the experimental values. It might be conducted that the origin of peak position and level width of quasi-free regions are not due to dynamical aspect but kinematical one. Our calculated quasi free Y-p and Y^*-p spectrum well reproduced the missing mass spectrum of E-27 experiment including the ΣN-ΛN conversion cusp in the Y-p region. In the proton coincidence spectrum, the broad enhancement was observed around the missing mass of 2270 MeV/c^2 which corresponds to a quasi-bound state of K^-pp. Our calculated missing-mass spectrum with the DISTO interaction well reproduced this broad bump structure.

Acknowledgements

I would like to thank Dr Tin Maung Hla, Rector, Mandalay University of Distance Education for his encouragement. I am grateful to the full support of Professor Dr Kay Thi New, Head of Department of Physics, Mandalay University of Distance Education . I am deeply indebted to Professor Dr Khin Swe Myint , Rector (Rtd.), Emeritus Professor, Department of Physics, University of Mandalay for all her enthusiastic discussion, collaboration and encouragement. I also would like to thank Dr Theigin, Lecturer, University of Mandalay for her discussion and collaboration.

References

1. Akaishi, Y., & Yamazaki, T. (1999). Proc. Daphne Workshop, Frascati Physics Series XVI , p. 59; to appear in Phys. Rev. C.
2. Agnello, M. *et al*., (2005). Phys. Rev. Lett **94** 212303.
3. Akaishi, Y., & Yamazaki, T. (2002). Phys. Rev. **C 65** 044005.
4. Akaishi, Y., & Yamazaki, T. (2002). Phys. Lett. **B 535** 70.
5. Akaishi, Y., Dote, A., & Yamazaki, T. (2005). Phys. Lett. **B 613** 140.
6. Dote, A. *et al*., (2003). arXiv:nucl-th **1** 0310085.
7. Ikeda, Y., & Sato, T. (2007). Phys. Rev. **C 76** 035203.
8. Ichikawa, Y. *et al*., (2013). XV International Conference on Hardon Spectroscopy-Hardon.
9. Ichikawa, Y. *et al*., (2015). Prog. Theor. Exp. Phys**. 021D01**.
10. Shevchenko, N.V., Gal, A., & Mares, J. (2007). Phys. Rev. Lett. **98** 082301.
11. Yamazaki, T. *et al*., (2007). Phys. Rev. **C 76** 045201.
12. Yamazaki, T. *et al*., (2010). Phys. Rev. Lett **104** 132502.